# An Eigenvalue Extension to the Candlestick Analytic Space-Time Depletion Benchmark and Its Application to Monte Carlo Simulation

Gabriel Kooreman and David P. Griesheimer

*Naval Nuclear Laboratory, 814 Pittsburgh McKeesport Blvd, West Mifflin, PA 15122*
*gabriel.kooreman@unnpp.gov, david.griesheimer@unnpp.gov*

## INTRODUCTION

Over the past several years there has been renewed interest in formally characterizing the stability and convergence behavior of coupled-physics simulations for nuclear engineering applications ([1, 2, 3, 4, 5]). Recent work in this area has resulted in the development of several analytic and semi-analytic benchmark problems for coupled neutronics/thermal-hydraulics [6, 7] and neutronics/depletion [8, 9] calculations. Although these benchmarks are academic in nature (e.g., 1-dimension, 1-group, monodirectional, fixed-source), they provide a valuable resource for quantitatively assessing convergence and error propagation in multiphysics coupling algorithms and verifying code implementations of established methods. To our knowledge, all analytic and semi-analytic multiphysics benchmarks reported to date have involved fixed-source radiation transport. In this paper we consider the extension of an existing neutronics/depletion benchmark to an eigenvalue $k_{\text{eff}}$ radiation transport problem.

In 2018, Kooreman and Griesheimer [8] developed an analytic solution to a coupled space-time depletion calculation. The "Candlestick" depletion benchmark involves sequential burning of a 1-dimensional slab of purely absorbing material by a constant incident current of monoenergetic, monodirectional neutrons on one face of the slab. The slab material is homogeneous and includes a single purely absorbing nuclide with constant microscopic cross section. Neutron absorption events cause the constituent nuclide to be destroyed, without the creation of any secondary daughter nuclides. The resulting analytic solution for this benchmark shows that both the neutron flux and nuclide number density are described by a wavefront that propagates at constant velocity through the slab in the direction of the initial radiation source.

Interestingly, a 2018 paper by Bernede and Poëtte [9] found the same expression as the asymptotic solution to the Candlestick benchmark in their analytic solution of a non-linear depletion system without space dependence. While their benchmark does not require the quasi-static approximation, it also omits spatial dependence and does not include the initial transition of neutron flux from purely exponential to the asymptotic solution that occurs far from the slab boundary at early depletion times.

Multiphysics simulations typically involve coupled systems of non-linear partial differential equations, which generally do not have closed-form analytic solutions. In references [6, 7, 8, 9] analytic or semi-analytic solutions are made possible because the 1-D, purely absorbing, monodirectional nature of the benchmark models reduces the differential equation for radiation transport to an especially simple and convenient form. Unfortunately, the monodirectional flux characteristic of the previous benchmark problems cannot be used for non-trivial multiplying material (eigenvalue) problems, which require bi-directional connectivity between regions in the model. In this paper, we show that it is possible to adapt the original Candlestick benchmark into a related two-group problem where the solution in the thermal group is identical to the analytic solution from the original benchmark. The resulting eigenvalue Candlestick model uses highly-simplified physics (e.g., $S_2$ scattering and fission neutron emission) but preserves the important characteristics of a coupled eigenvalue-neutronics/depletion simulation and is useful for code verification and assessment of convergence properties and propagation of uncertainty in coupled calculations.

## EIGENVALUE CANDLESTICK BENCHMARK

### Benchmark Description

Consider a one-dimensional homogeneous slab of purely-fissioning fuel occupying $x = [0, L]$ with microscopic fission cross section $\sigma_{\text{f}}$ in the thermal group and no interactions in the fast group. The slab has initial constant number density $N_0$ at time $t = 0$. To the left of the slab is some perfect neutron moderator that acts by returning all exiting fast neutrons as entering thermal neutrons, and to the right of the slab is vacuum, as shown in Fig. 1.

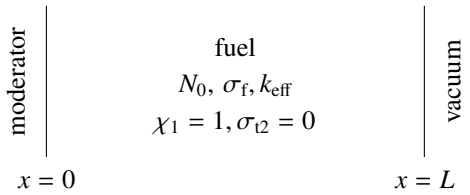


Fig. 1. Illustration of benchmark geometry

Because the timescale of neutron streaming and precursor decay is significantly shorter than that of fuel depletion, the quasi-static approximation is applied to the transport equation by setting the $\frac{1}{v}\frac{\partial \psi}{\partial t}$ term to zero. The use of the quasi-static approximation is consistent with traditional reactor depletion calculations as well as with the previous Candlestick benchmark problem [8]. In order to enforce the quasi-static condition, a time-dependent normalization factor $k_{\text{eff}}(t)$ is applied to the fission neutron yield, $\nu$. Note that the normalization factor is equivalent to the $k$-eigenvalue traditionally used in reactor neutron transport calculations.

If neutrons are restricted to travel only along the $x$ axis, then the system can be described by the following non-linear system of equations for angular flux and number density,

$$\frac{\partial \psi_1^-(x,t)}{\partial x} = -\frac{\nu\sigma_{\text{f}}}{2k_{\text{eff}}(t)} N(x,t)\psi_2^+(x,t), \quad \psi_1^-(L,t) = 0, \quad \text{(1a)}$$

$$\frac{\partial \psi_2^+(x,t)}{\partial x} = -\sigma_f N(x,t)\psi_2^+(x,t), \quad \psi_2^+(0,t) = \psi_1^-(0,t), \quad (1b)$$

$$\frac{\partial N(x,t)}{\partial t} = -\sigma_f N(x,t)\psi_2^+(x,t), \quad N(x,0) = N_0. \quad (1c)$$

In these equations, group 1 refers to the fast group, group 2 refers to the thermal group, and the superscripts $^+$ and $^-$ refer to the forward and backward direction, respectively. Fast neutrons traveling in the positive direction do not interact with this material and so are omitted from the system of equations. Likewise, there are no thermal neutrons traveling in the $-x$ direction. In addition to the transport and depletion equations shown in Eqs. 1 the magnitude of the flux is determined by a power normalization condition, typically stated as

$$P(t) = q \int_0^L \sigma_f \psi_2^+(x,t) \mathrm{d}x, \quad (2)$$

where $P$ is the total power output of the slab and $q$ is the constant energy release per fission event.

The equations for transport and depletion involving thermal neutrons (Eqs. 1b and 1c) are nearly identical to the governing equations for the original fixed-source Candlestick depletion benchmark. In fact, the only difference between the equations for the fixed-source and eigenvalue problems lies in the thermal flux boundary condition at the left edge, $\psi_2^+(0,t)$. In the fixed-source benchmark this boundary condition is a constant value for all times, representing the external source of neutrons incident on the slab. In the eigenvalue benchmark, the incident thermal flux on the left side of the slab depends on the fission rate in the slab, and can be written

$$\psi_2^+(0,t) = \frac{1}{2} \int_0^L \frac{\nu\sigma_f}{k_{\text{eff}}(t)} \psi_2^+(x,t) \mathrm{d}x, \quad (3)$$

where we have assumed that all neutrons produced in fission are equiprobably born in either the forward or backward direction (an $S_2$ source). Taking the ratio of Eqs. 3 and 2 yields an expression for the incident thermal flux as a function of reactor power and the multiplication factor, $k_{\text{eff}}$,

$$\psi_2^+(0,t) = \frac{\nu}{2q} \frac{P(t)}{k_{\text{eff}}(t)}. \quad (4)$$

In many reactor depletion applications, the power level $P$ in Eq. 2 is assumed to be constant. Under this assumption it follows from Eq. 4 that the magnitude of the incident thermal flux at $x = 0$ will increase as the multiplication factor of the slab decreases due to fuel burnup. Unfortunately, the analytic solution from the original Candlestick benchmark does not apply for a time-dependent incident flux condition, nor is an analytic solution known for this condition. Therefore, we seek to modify the eigenvalue benchmark model to enforce that the incident thermal flux at $x = 0$ remains constant for all times. This causes the thermal group of the eigenvalue benchmark to reduce to an identical form as the fixed-source benchmark, enabling reuse of the original analytic solution. This objective can be achieved by assuming that the power level of the slab decreases over time in proportion to the multiplication factor for the system

$$P(t) = P_0 \frac{k_{\text{eff}}(t)}{k_{\text{eff}}(0)}, \quad (5)$$

where $P_0$ is the initial (reference) power for the slab. Note that substituting Eq. 5 into Eq. 4 yields a time-independent incident thermal flux condition of $\psi_2^+(0,t) = \nu P_0 / 2q k_{\text{eff}}(0)$, as desired. Using Eq. 5 as the power normalization condition in place of Eq. 2 causes the equations for the thermal group in the eigenvalue formulation to reduce to the same form as the original fixed-source depletion benchmark.

As shown in the next Section, Eqs. 1 can be solved to yield analytic forms for the fast and thermal flux, fuel number density, $k_{\text{eff}}(t)$, and the time-dependent slab power $P(t)$. Interestingly, numerical solutions for the benchmark require $P(t)$ as an input condition and, therefore, must use the analytic result for the time-varying power level as a part of the input definition for the benchmark. Thus, the eigenvalue Candlestick benchmark is similar to benchmarks developed via the method of manufactured solutions in the sense that reproduction of the analytic solution requires a specific, and well-defined, input condition.

### Benchmark Solution

Solution of the eigenvalue Candlestick depletion benchmark problem begins by recognizing that the time dependent power normalization in Eq. 5 ensures a constant left boundary condition for thermal flux in the slab. Under this normalization Eqs. 1b and 1c become decoupled from Eq. 1a and take the form of the fixed source Candlestick benchmark problem, for which an analytic solution is known [8]. The solution for $\psi_2^+(x,t)$ and $N(x,t)$ is

$$\psi_2^+(x,t) = \frac{\frac{\nu P_0}{2q k_{\text{eff}}(0)} e^{\Sigma_{f0}\gamma t}}{e^{\Sigma_{f0}\gamma t} + e^{\Sigma_{f0} x} - 1}, \quad (6a)$$

$$N(x,t) = \frac{N_0 e^{\Sigma_{f0} x}}{e^{\Sigma_{f0}\gamma t} + e^{\Sigma_{f0} x} - 1}, \quad (6b)$$

where $\Sigma_{f0} \equiv \sigma_f N_0$ is the initial macroscopic fission cross section and $\gamma \equiv \frac{\nu P_0}{2q k_{\text{eff}}(0) N_0}$ is the depletion wavefront propagation velocity.

By applying Eqs. 6 to Eq. 1a, the fast flux and eigenvalue can be determined through integration to be

$$\psi_1^-(x,t) = \frac{\nu^2 P_0 e^{\Sigma_{f0}\gamma t}}{4q k_{\text{eff}}(0) k_{\text{eff}}(t)} \left[ \frac{1}{e^{\Sigma_{f0} x} + e^{\Sigma_{f0}\gamma t} - 1} - \frac{1}{e^{\Sigma_{f0} L} + e^{\Sigma_{f0}\gamma t} - 1} \right], \quad (7a)$$

$$k_{\text{eff}}(t) = \frac{\nu e^{\Sigma_{0f}\gamma t}}{2} \left[ e^{-\Sigma_{f0}\gamma t} - \frac{1}{e^{\Sigma_{f0} L} + e^{\Sigma_{f0}\gamma t} - 1} \right]. \quad (7b)$$

## NUMERICAL RESULTS

The solutions presented above are closed-form analytic expressions, and, as such, they are valid for any physical choice of parameters. In order to test the benchmark against a numerical solution, some arbitrary values are chosen for the physical parameters present. The values in Table I were chosen because they roughly match the (magnitude of) values that would be expected of an operating nuclear reactor. These parameters lead to the solution for eigenvalue as a function of time given in Fig. 2.

TABLE I. Parameters for eigenvalue Candlestick benchmark

| Parameter | Value |
|---|---|
| Initial Power ($P_0$) | 2 MW |
| Initial density ($N_0$) | 2 $\frac{\text{atom}}{\text{b·cm}}$ |
| Slab thickness ($L$) | 3 cm |
| Maximum time ($t_{\max}$) | 3.3 yrs |
| Fission xs ($\sigma_f$) | 1.3 b |
| Neutron multiplicity ($\nu$) | 2.5 |

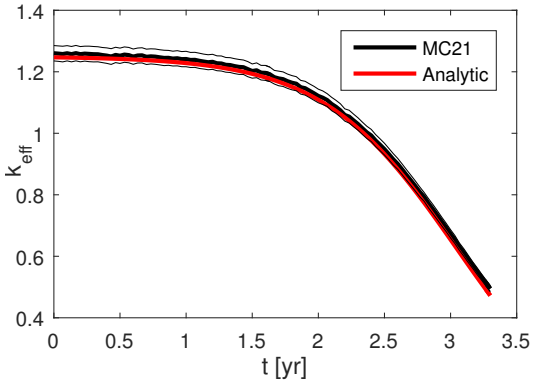


Fig. 2. Solution for $k_{\text{eff}}(t)$ using the parameters in Table I. MC21 95% confidence interval depicted with lighter-weight lines. MC21 calculation performed with $1{\times}10^6$ histories, 75 time steps, and a second-order scheme in time.

### Monte Carlo Implementation

The eigenvalue Candlestick benchmark was implemented in the MC21 Monte Carlo code [10]. The fuel was modeled as a 3×1×1 cm parallelepiped divided into 100 equal-sized compositions along the $x-$dimension. The fuel material includes a fictitious purely-fissioning nuclide with $\sigma_{t,1} = 0$ b, $\sigma_{t,2} = \sigma_{f,2} = 1.3$ b, and $\nu = 2.5$. Neutrons produced by fission of this nuclide are always emitted in group 1 ($E > 0.625$ eV) with $\mu = \pm 1$ with respect to the $x$-axis. Adjacent to the fuel slab is a 5×1×1 cm parallelepiped containing a moderator material that consists of a fictitious purely-scattering nuclide with $\sigma_{t,1} = \sigma_{s,1} = 1300$ b and $\sigma_{t,2} = 0$ b. Scattering events with the fictitious nuclide produce an exiting neutron in group 2 ($E < 0.625$ eV) with direction within 1° of the $x$-axis (corresponding to a scattering cosine distribution of $\mu \in [-1, -0.9999], [0.9999, 1]$).

Reflecting boundary conditions are applied to all outer surfaces except the outer fuel surface (right face of the slab) which has a vacuum boundary. The density of the moderator material is set to $1 \times 10^5$ atoms/b·cm, which gives an effective mean free path of $7.69 \times 10^{-9}$ cm for fast neutrons in the moderator. As a result, the optical thickness of the moderator is equal to $13{\times}10^9$ mean free paths (accounting for reflection), which ensures that all fast neutrons will scatter and thermalize in the moderator material.

Fuel depletion was performed using the built-in MC21 depletion solver [10] with either a first-order (constant flux) or second-order predictor-corrector discretization scheme in time. All of the following calculations used a running strategy involving 150 batches of $10^3$ histories each unless stated otherwise. The time-dependent power level was evaluated using the analytic power formula given in Eq. 5. When a first-order time discretization was used, the instantaneous power at the beginning of the time step (BOT) was used to normalize the neutron flux and reaction rates over the time step. When a second-order scheme in time was used, the instantaneous power at BOT and end of time step (EOT) were used to normalize the nuclide reaction rates at the corresponding times. During the depletion solve, the change in nuclide reaction rate over the time step was approximated as a linear interpolation between the BOT and EOT conditions.

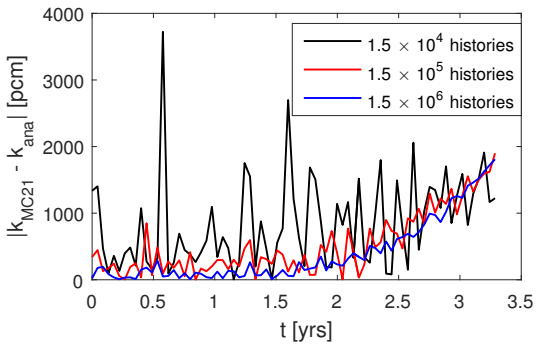


Fig. 3. Error in eigenvalue of MC21 solution as a function of time for different numbers of histories when 75 time steps are used with a second-order scheme in time.

Note that both first- and second-order methods include an approximation (constant or linear) to account for the time-dependence of the slab power level during a time step, which introduces a source of numerical error in the time discretization of the depletion equations. A similar discretization error occurs in constant power depletion calculations due to the change in flux magnitude and spectrum during the time step, which is caused by fuel depletion, build-up of fission product poisons, and external changes in reactivity.

### Convergence of Monte Carlo Simulation

In Figs. 3, 4, and 5, the MC21-calculated eigenvalue is compared against the analytic solution as a function of time. The effect of the number of histories used per transport update is presented in Fig. 3. As seen in the figure, the error in the eigenvalue tends to rise as the eigenvalue falls. Interestingly, the trend of the error is the same regardless of the number of histories used in the calculation. This result suggests that the increased trend of eigenvalue error is not due to an accumulation of stochastic error over many time steps. In this case, the error trend is likely due poorer behavior of the spatial discretization when the total optical thickness of the slab becomes very thin.

The remaining two plots, Figs. 4 and 5 present the effect of time discretization on this MC21 implementation of the eigenvalue Candlestick benchmark. In Fig. 4, the effect of using a first order or second order time discretization for the

depletion step (as well as for evaluating the analytic power expression) is shown. As expected, the second order scheme is significantly more accurate, and this accuracy difference is amplified with time. Fig. 5 illustrates the eigenvalue error for three different time step sizes for a second-order discretization. As expected, the eigenvalue error is much higher when only 15 time steps are used than when 75 time steps are used. Note that the error when using only 15 time steps with the second order scheme is still much less than the error when using 75 time steps with a first order scheme. This suggests that first order schemes are inadequate for long-lived depletion calculations unless $\Delta t$ is made unreasonably small. Also note that the accuracy does not improve from 75 to 500 time steps. This is likely due to the fact that all of these cases use the same spatial discretization for the depletion compositions (100 cells between 0 and L), suggesting that the error is dominated by the effect of spatial discretization once the time discretization includes at least 75 time steps.

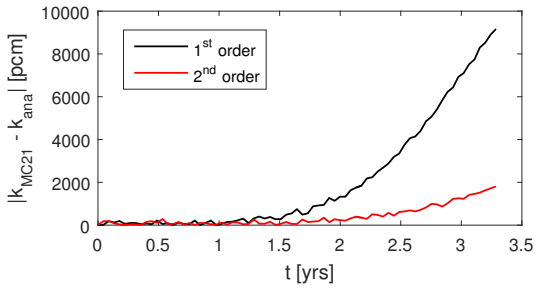


Fig. 4. Error in eigenvalue of MC21 solution as a function of time for first or second-order time stepping, when 75 total time steps are used.

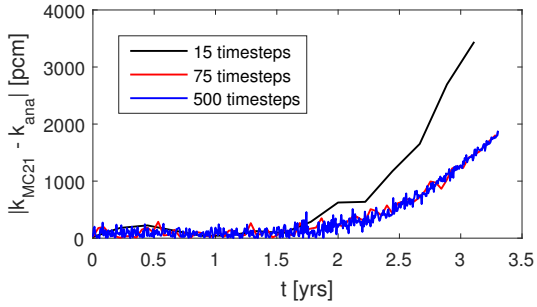


Fig. 5. Error in eigenvalue of MC21 solution as a function of time for different number of time steps taken in the calculation.

## CONCLUSIONS

In this summary, an eigenvalue version of the Candlestick benchmark problem for space-time reactor depletion calculations is presented. By reducing the slab power over time according to the formula given in Eq. 5, the solution for thermal flux and number density can be shown to be identical to that of the fixed-source Candlestick benchmark problem. This allows calculation of a closed-form and analytic solution for thermal flux, fast flux, number density, and eigenvalue. The eigenvalue Candlestick benchmark problem is appropriate for analyzing most space-time depletion codes and can lead to insight into the accuracy of these codes. As an example of this, the benchmark was run with the MC21 Monte Carlo code and used for a few simple tests of convergence of depletion problems. In particular, it was demonstrated that over many time steps, the solution accuracy is not a strong function of the number of histories used, indicating that stochastic errors do not tend to accumulate over time for this case.

## REFERENCES

1. J. DUFEK and J.E. HOOGENBOOM, "Numerical Stability of Existing Monte Carlo Burnup Codes in Cycle Calculations of Critical Reactors," *Nucl. Sci. Eng.*, **162**, 307–311 (2009).
2. J. DUFEK ET AL., "Numerical Stability of the Predictor Corrector Method in Monte Carlo Burnup Calculations of Critical Reactors," *Ann. Nucl. Energy*, **56**, 34 (2013).
3. J.D. DENSMORE, D.F. GILL, and D.P. GRIESHEMER, "Stability Analysis of Burnup Calculations," *Trans. Am. Nuc. Soc.*, **108**, 695 – 698 (2013).
4. Q. NEWELL and C. SANDERS, "Stochastic Uncertainty Propagation in Monte Carlo Depletion Calculations," *Nucl. Sci. Eng.*, **179**, 253 (2015).
5. D.F. GILL, D.P. GRIESHEIMER, and D.L. AUMILLER, "Numerical Methods in Coupled Monte carlo and Thermal-Hydraulic Calculations," *Nuc. Sci. Eng.*, **185**, 194 – 205 (2015).
6. J. WANG and W. MARTIN, "Verification of a Multiphysics code with a Method of Manufactured Solutions," *Trans. Am. Nuc. Soc.*, **116**, 1116–1119 (2017).
7. D.P. GRIESHEIMER, D.L. AUMILLER, and D.F. GILL, "Proposed Semi-Analytic Benchmark for Coupled Neutronics/Thermal-Hydraulics Feedback in Multiphysics Simulations," *Trans. Am. Nuc. Soc.*, **116**, 1285 – 1289 (2016).
8. G. KOOREMAN and D. P. GRIESHEIMER, "A Fully Analytic Space-Time Depletion Benchmark and its Applications to Monte Carlo Simulation," in "Proc. PHYSOR 2018: Reactor Physics paving the way towards more efficient systems," Cancun, Mexico (2018).
9. A. BERNEDE and G. POETTE, "An Unsplit Monte-Carlo solver for the resolution of the linear Boltzmann equation coupled to (stiff) Bateman equations," *J. Comp. Phys.*, **354**, 211–241 (2018).
10. D.P. GRIESHEMER ET AL., "MC21 v6.0 – A Continuous-Energy Monte Carlo Particle Transport Code with Integrated Reactor Feedback Capabilities," *Ann. Nucl. Energy*, **82**, 29 – 40 (2015).